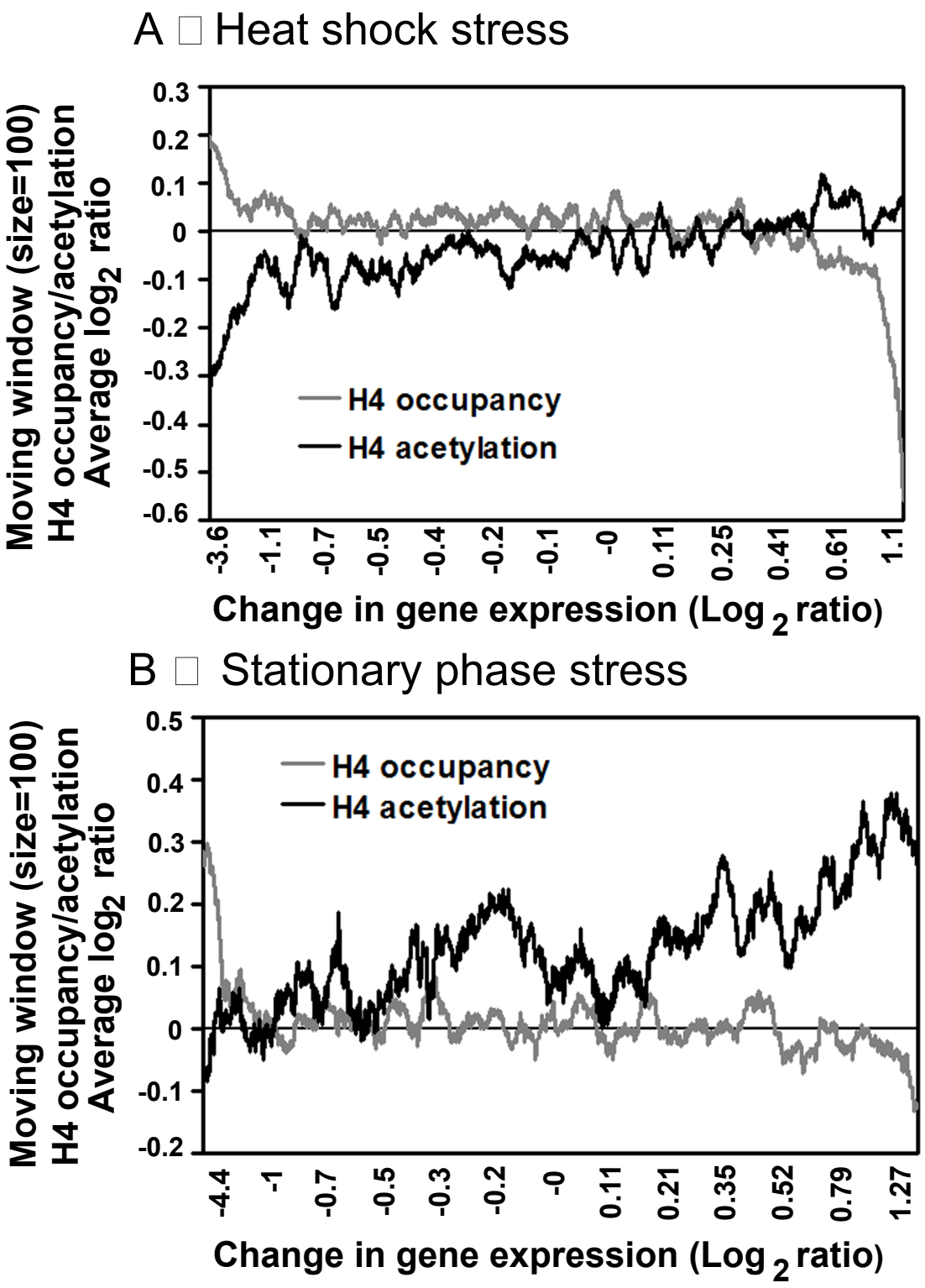

Supplementary Figure S1:
Promoter histone occupancy and downstream gene expression are inversely correlated:
A moving window average (window size 100, step size 1) applied to the y-axis shows the global relationships between histone H4 occupancy, Acetylated histone H4 levels and change in gene expression after (*A*) Heat shock, and (*B*) stationary phase stress.

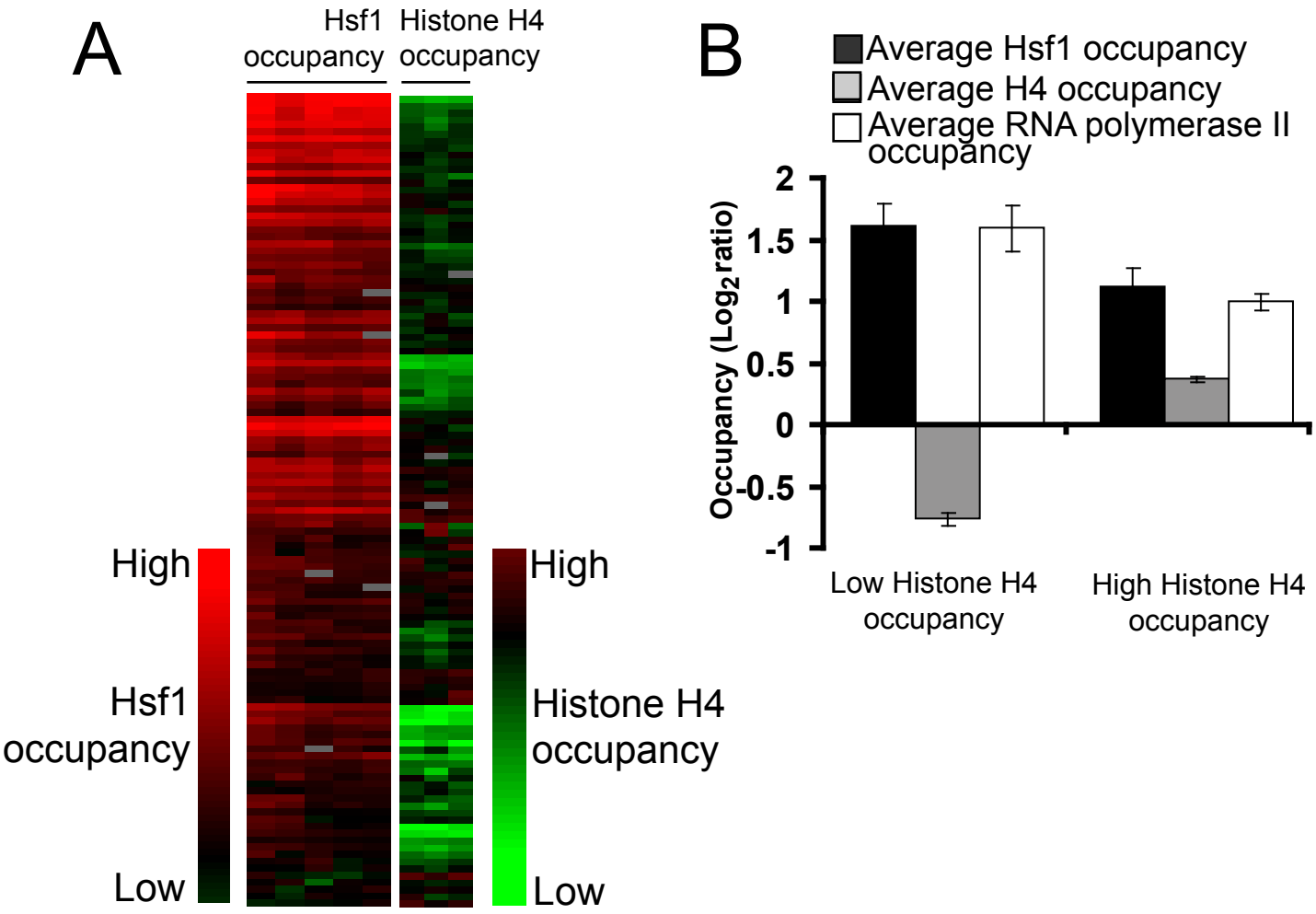

Supplementary Figure S2:
Hsf1 occupancy at its target promoters in unstressed cells is inversely correlated to promoter histone H4 occupancy.
(*A*) Red-green heat maps comparing Hsf1 occupancy and histone H4 occupancy at the Hsf1 target genes during unstressed conditions in yeast. The Hsf1 occupancy data is from a previously published work (Hahn et al 2004) and shows five independent data sets. The histone H4 occupancy is from the current study and is from three independent biological replicates.
(*B*) Binding of Hsf1 to target promoters results in loss of nucleosomes at the promoter region and poises genes for transcription as seen by increase in RNA polymerase II occupancy. The Hsf1 target promoters were sorted from low to high histone H4 occupancy at 30^{o}C and the promoters were divided into four quartiles. The average histone H4 occupancy in the first quartile was plotted against the average histone H4 occupancy in the fourth quartile along with the average Hsf1 occupancy and the average RNA pol II occupancy from Radonjic et al. Molecular Cell, 2005. The graph shows that the promoters containing high H4 occupancy have comparatively lower Hsf1 binding and and those having low H4 occupancy have higher Hsf1 binding. The graph also shows that high Hsf1 occupancy correlates with high RNA Pol II occupancy.

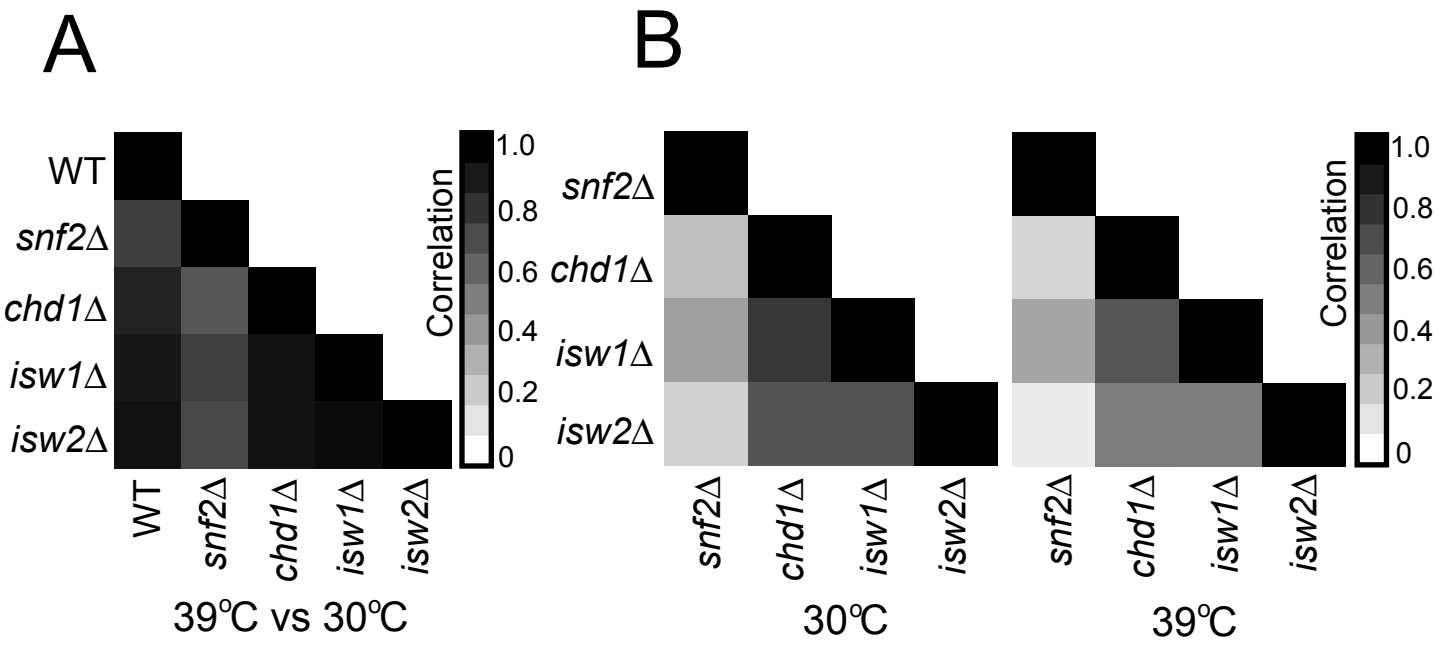

Supplementary Figure S3:
Snf2 has a role in heat shock stress response:
The genome wide expression changes in yeast strains containing deletions in subunits of four ATP-dependent chromatin remodelers and in WT cells were compared using microarray analysis. The pair-wise Pearson's correlation was calculated for each of the mutants and the WT cells.
(*A*) A matrix depicting the degree of correlation between expression levels of genes in the deletion strains and WT cells when subjected to heat shock stress. Expression change in *snf2*Δ cells correlate least with WT cells. The scale indicates the degree of correlation and the diagonal is the correlation expression in each cell to itself. The correlation between biological replicates of the WT and the different mutant cells were between 0.895 and 0.96, therefore are not shown, in order to simplify the matrix.
(*B*) Correlation matrices comparing different deletion strains at 30°C (left) and at 39°C (right).

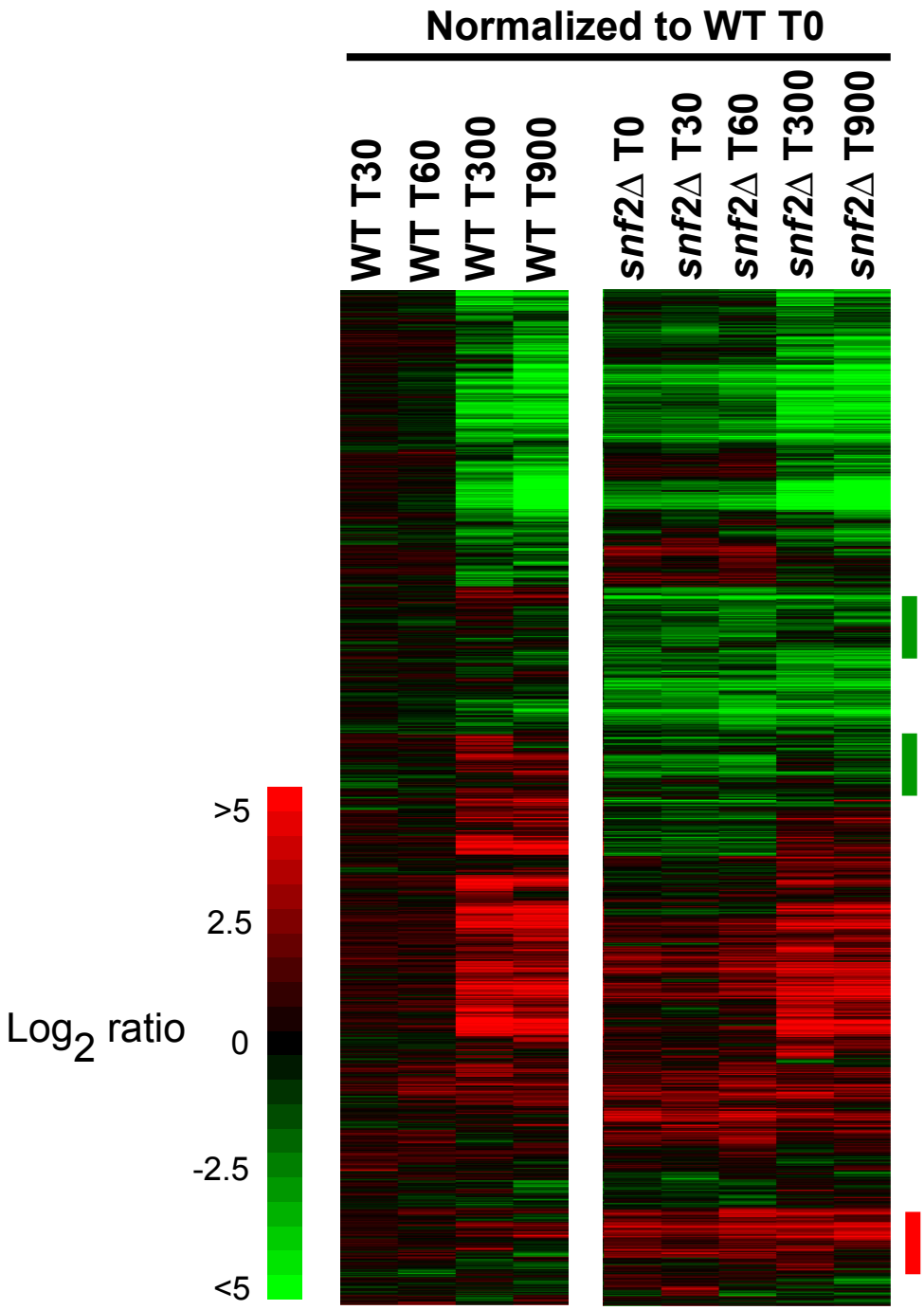

Supplementary Figure S4:
Whole-genome expression profiles from the time course experiment in WT and *snf*2Δ cells. Cells were subjected to heat shock stress and harvested at time points 0s, 30s, 60s, 300s and 900s. mRNA was extracted and hybridized onto DNA microarrays against a control mRNA. The red-green heat map was generated by dividing the ratios at all the time points with ratio from time point T0 of WT cells followed by hierarchical clustering.Green bars mark the genes that show upregulation in WT cells, but do not show upregulation in *snf*2Δ cells. Red bar marks the genes that are upregulated more than WT levels in *snf*2Δ cells.

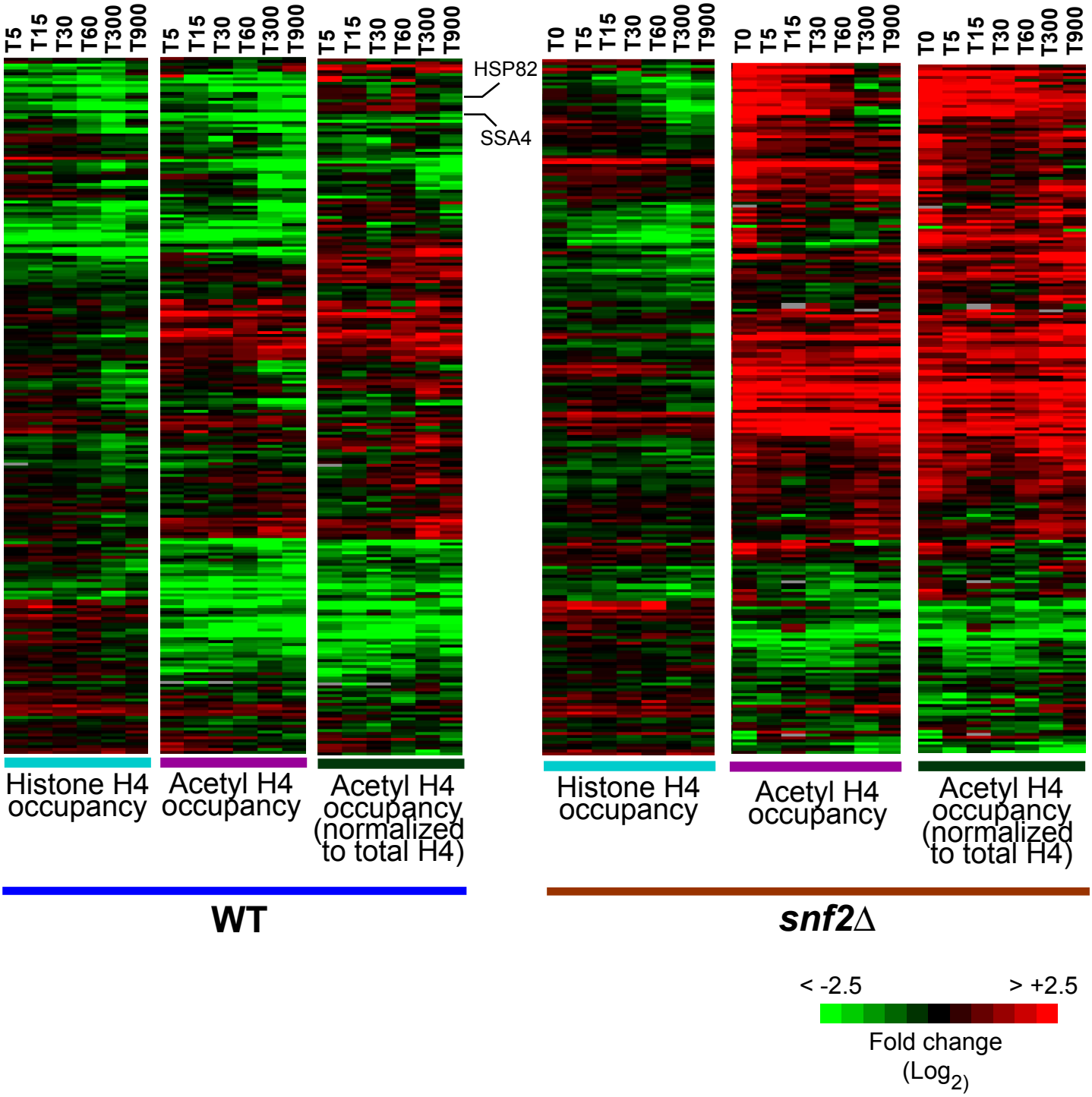

Supplementary Figure S5:

Kinetics of histone H4 occupancy and acetylated histone H4 occupancy changes during heat shock. Genes whose expression was upregulated 2.5 fold or more by heat shock were clustered hierarchically. The heat maps show the kinetics of histone H4 loss and acetylated histone H4 loss after heat shock in WT and *snf2*Δ cells. All the time points are compared to WT T0 time point.